Shortest Coordinated Motion for Square Robots

Guillermo Esteban[1,2(✉)], Dan Halperin[3], Víctor Ruíz[4], Vera Sacristán[4], and Rodrigo I. Silveira[4]

[1] Departamento de Física y Matemáticas, Universidad de Alcalá, Alcalá de Henares, Spain
g.esteban@uah.es
[2] School of Computer Science, Carleton University, Ottawa, Canada
[3] School of Computer Science, Tel Aviv University, Tel Aviv, Israel
[4] Departament de Matemàtiques, Universitat Politècnica de Catalunya, Barcelona, Spain

Abstract. We study the problem of determining minimum-length coordinated motions for two axis-aligned square robots translating in an obstacle-free plane: Given feasible start and goal configurations, find a continuous motion for the two squares from start to goal, comprising only robot-robot collision-free configurations, such that the total Euclidean distance traveled by the two squares is minimal among all possible such motions. We present an adaptation of the tools developed for the case of discs by Kirkpatrick and Liu [*Characterizing minimum-length coordinated motions for two discs*. Proceedings 28th CCCG, 252-259, 2016; CoRR abs/1607.04005, 2016.] to the case of squares. Certain aspects of the case of squares are more complicated, requiring additional and more involved arguments over the case of discs. Our contribution can serve as a basic component in optimizing the coordinated motion of two squares among obstacles, as well as for *local planning* in sampling-based algorithms, which are often used in practice, in the same setting.

Keywords: Motion planning · Coordinated motions · Geometric algorithms

1 Introduction

The basic motion planning problem is, given start and goal placements for moving objects (robots), to decide whether the objects can move from start to goal without colliding with obstacles in the environment nor with one another, and

Partially supported by project PID2019-104129GB-I00/MCIN/AEI/10.13039/501100011033 of the Spanish Ministry of Science and Innovation. Work by D.H. has been supported in part by the Israel Science Foundation (grant no. 1736/19), by NSF/US-Israel-BSF (grant no. 2019754), by the Israel Ministry of Science and Technology (grant no. 103129), by the Blavatnik Computer Science Research Fund, and by the Yandex Machine Learning Initiative for Machine Learning at Tel Aviv University.

P. Morin and S. Suri (Eds.): WADS 2023, LNCS 14079, pp. 430–443, 2023.
https://doi.org/10.1007/978-3-031-38906-1_28

if so, to plan such a motion. This problem has been intensively investigated for almost five decades now; see, e.g., several books and surveys [1,4,5,9,11,15]. The basic problem is relatively well understood, has general theoretical solutions as well as an arsenal of more practical approaches used by practitioners in robotics, molecular biology, animation, computer games, and additional domains where one needs to automatically plan or simulate feasible collision-free motions; see, e.g., [10].

Finding a feasible collision-free motion is typically insufficient in practice, and we aim to find paths of high quality, such as short paths, paths with high clearance from obstacles, paths requiring minimum energy and so on. Optimizing motion plans is in general significantly harder than finding a feasible solution. The topic is discussed in the books and surveys mentioned above; the specific topic of geometric shortest path problems is reviewed in [13].

1.1 Optimal Motion in the Absence of Obstacles

Let $\mathbb{A}$ and $\mathbb{B}$ be two axis-aligned square robots in the plane. The position of robot $\mathbb{A}$ (resp., $\mathbb{B}$) at a given moment is denoted by A (resp., B), and refers to the coordinates of its center. We define the *radius* of a square as the length of its apothem (half an edge, in the case of a square). Let $r_{\mathbb{A}}$ and $r_{\mathbb{B}}$ be the radii of robot $\mathbb{A}$ and robot $\mathbb{B}$, respectively, then we define $r = r_{\mathbb{A}} + r_{\mathbb{B}}$. The movement of robot $\mathbb{A}$ in the presence of robot $\mathbb{B}$ can be described as the movement of the point A in the presence of robot $\mathbb{B}'$ with radius r. Thus, from this point on, for convenience of exposition, we will assume that one robot is shrunk to a point and the other robot has the expanded radius r.

Given a point X in the plane, we denote by $sq(X)$ the open axis-aligned square centered at X, with radius r.

We say that a pair of positions (A, B) is *feasible* if $A \notin sq(B)$. Notice that this implies that $B \notin sq(A)$. An *instance* of our problem consists of a feasible pair of initial and final positions (A_0, B_0) and (A_1, B_1), respectively. A *trajectory* from a point X_0 to a point X_1 in the plane is any continuous rectifiable curve $m_X : [0, 1] \to \mathbb{R}^2$ such that $m_X(0) = X_0$ and $m_X(1) = X_1$. Given an instance of our problem, a *coordinated motion* m is a pair of trajectories $m = (m_A, m_B)$. Throughout this paper we refer to *coordinated motions* simply as *motions*. A motion is *feasible* if for all $t \in [0, 1]$ the pair of positions $m(t) = (m_A(t), m_B(t))$ is feasible. We denote the Euclidean arc-length of a trajectory m_X by $\ell(m_X)$. We define the *length* of a motion $m = (m_A, m_B)$ as $\ell(m) = \ell(m_A) + \ell(m_B)$. We focus in this paper on minimum-length coordinated translational motion for two squares. Our goal is to find a description of a minimum-length feasible motion (m_A, m_B), for each instance of the problem. An example of an optimal coordinated motion for two square robots is shown in Fig. 1. We note that, in the figures of this paper, squares representing robots are drawn with filled color, while squares $sq(X)$ are depicted with a white filling.

Feasible motion for two squares translating among polygonal obstacles with n vertices can be found in $O(n^2)$ time, if one exists [16]. For an arbitrary number of unit squares in the same setting, the problem is known to be PSPACE-

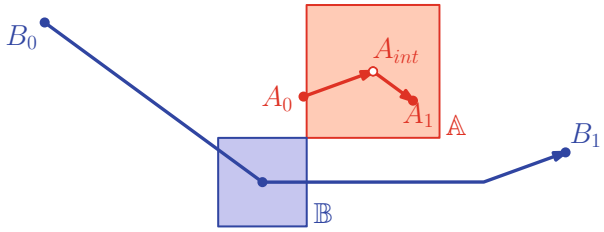

Fig. 1. Example of an optimal motion: first, $\mathbb{A}$ is translated from A_0 to A_{int}, then $\mathbb{B}$ moves from B_0 to B_1 avoiding $\mathbb{A}$, finally, $\mathbb{A}$ is translated from A_{int} to A_1. The squares show the positions of the two robots when $\mathbb{A}$ is at A_{int} and $\mathbb{B}$ is starting to slide around $\mathbb{A}$.

hard [17]. Recently, Kirkpatrick and Liu [7,8] solved the minimum-length coordinated motion for two discs, as we discuss below in Sect. 1.2.

We remark that optimal motion in the absence of obstacles was also investigated for a single wheeled vehicle; see, for example, the work by Dubins [2], or by Reeds and Shepp [14]. The major complication in deriving optimal paths for such systems even in the absence of obstacles stems from their being non-holonomic. The resulting paths bear some similarity to the results obtained in [7] and in the current paper in that the optimal motion of a single robot/vehicle comprises a small set of simple primitive paths. For more details and additional references, see [11, Section 15.3].

1.2 The Kirkpatrick-Liu Analysis for Two Discs

Kirkpatrick and Liu [7,8] describe, for any pair of initial and final positions of the discs, two motions that involve at most six (straight or circular-arc) segments. Then, either (i) a single motion is feasible and optimal, or (ii) among the two motions, one is optimal among all clockwise[1] motions and the other is optimal among all counterclockwise motions. The proof of the optimality of the motions involves an extensive case analysis, which depends on the relative initial and final positions of the discs. However, all motions have a simple structure:

1. Move robot $\mathbb{A}$ from its initial position to an intermediate position A_{int}.
2. Move robot $\mathbb{B}$ from its initial position to its final position.
3. Move robot $\mathbb{A}$ from the intermediate position A_{int} to its final position.

The main mathematical tool employed in [7,8] is *Cauchy's surface area formula*. Its use in the context of optimal motion planning was introduced by Icking et al. [6] for a line segment translating and rotating in the plane. The study of the full rigid motion of a segment involves rotation, which raises the question how to measure the distance between two configurations of the moving object.

[1] Formally defined in Sect. 2; roughly, clockwise here refers to the direction of rotation of a vector from the center of one robot to the center of the other robot throughout the motion, from start to goal.

Icking et al. [6] focus on what they call the d_2-distance, which measures the length of the motion of a segment $\overline{pq}$ by averaging the distance travelled by its two endpoints p and q. We remark that the case of a segment has attracted much attention—the interesting history of the problem, as well as other distance measures, are reviewed in [6].

There is a close relation between minimizing the d_2-distance traveled by a segment and the minimum-length coordinated motion of two discs. Assume the sum of the radii of the two discs equals the length $|pq|$ of the segment. Then, if the two discs remain in contact throughout the whole motion, the two problems are equivalent.

In this paper, we adapt the techniques from [7,8] to square robots. Our work for squares makes several contributions beyond the work for discs. Primarily, as we explain below, there are certain complications for squares that do not arise with discs, making the analysis more complex. Secondly, we complete details that are similar to both systems but have not been dealt with previously. For square robots the shape and relative position matters. The square corners create discontinuities in tangency points, which impacts the definition of the cases that need to be analyzed. The relative position of the two squares (more precisely, the slope of the line passing through the centers of the two squares) also has to be taken into account. For example, the possible shapes of optimal motions can vary considerably between horizontally-aligned and non-horizontally-aligned squares, giving rise to situations that do not exist for disc robots. Additionally, when a disc slides along the boundary of another disc, the distance between their centers remains constant, as opposed to the case for squares, where the distance varies with the angle of contact. This forces us to derive new conditions that guarantee the optimality of motions.

Optimal motion planning for two squares is a fundamental problem. As mentioned above, in the presence of obstacles, we do not even know if the problem has a polynomial-time solution. Understanding the obstacle-free case is a first significant step toward devising solutions to the more complex case with obstacles. Also, these results could serve as good *local motion plans* [11], for more practicable solutions based on sampling.

2 The General Approach

In this section we present the general framework to prove that a motion is optimal, based on the work by Kirkpatrick and Liu [7,8] and Icking et al. [6].

The *trace* of a trajectory m_X is defined as the image of m_X in the plane. For the remaining of this paper, we will use the notation m_X to refer to a trajectory m_X and its trace. Let $\overline{m}_X$ be the boundary of the convex hull of m_X. The trajectory m_X is said to be *convex* if $\overline{m}_X = m_X \cup \overline{X_0X_1}$, where $\overline{X_0X_1}$ is the segment whose endpoints are $m_X(0) = X_0$ and $m_X(1) = X_1$.

A motion $m = (m_A, m_B)$ from (A_0, B_0) to (A_1, B_1) is optimal if both m_A and m_B are convex, and $\ell(\overline{m}_A) + \ell(\overline{m}_B)$ is minimized over all motions from (A_0, B_0) to (A_1, B_1), see [8, Lemma 3.1]. The convexity of m_A and m_B is easy to verify, but the minimality of $\ell(\overline{m}_A) + \ell(\overline{m}_B)$ is not. In order to facilitate proving optimality,

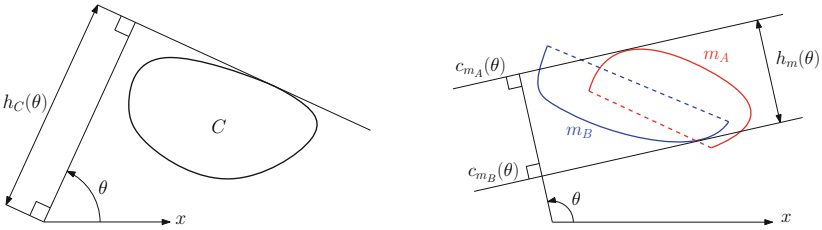

Fig. 2. Left: support function $h_C(\theta)$ of a closed curve C. Right: support function $h_m(\theta)$ of a motion $m = (m_A, m_B)$.

the problem of measuring $\ell(\overline{m}_A) + \ell(\overline{m}_B)$ can be translated into the problem of computing the width of a strip defined by a pair of *supporting lines*, one for $\overline{m}_A$ and one for $\overline{m}_B$ [6]. Given a closed curve C, its *support function* $h_C(\theta)$ can be seen as the (signed) distance from the origin to the extremal supporting line of C in the direction $\theta + \pi/2$. See Fig. 2a for an illustration. As noted in [6], Cauchy's surface area formula [3] implies that if C_1 and C_2 are two closed convex curves, then $\ell(C_1) + \ell(C_2) = \int_0^{2\pi} (h_{C_1}(\theta) + h_{C_2}(\theta + \pi))d\theta$.

We define $h_{m_A}(\theta)$ (resp., $h_{m_B}(\theta)$) to be the support function of $\overline{m}_A$ (resp., $\overline{m}_B$). Then $h_m(\theta) = h_{m_A}(\theta) + h_{m_B}(\theta + \pi)$ can be interpreted as follows. For each $\theta \in S^1$, let $c_{m_A}(\theta)$ be the supporting line for $\overline{m}_A$ in direction $\theta + \pi/2$ and $c_{m_B}(\theta)$ the supporting line for $\overline{m}_B$ in direction $\theta + \pi + \pi/2$. Then $h_m(\theta)$ is the width of the strip formed by the two supporting lines at the given angle, as illustrated in Fig. 2b.

Given two points X, Y, we define $\angle(X, Y)$ as the angle that vector $\overrightarrow{YX}$ forms with the positive x-axis. Let $\theta_0 = \angle(A_0, B_0)$ and $\theta_1 = \angle(A_1, B_1)$. If I is the range of angles $\angle(m_A(t), m_B(t))$ for all $t \in [0, 1]$, then either $[\theta_0, \theta_1] \subseteq I$ or $S^1 \backslash [\theta_0, \theta_1] \subseteq I$ (or both), due to the continuity of the trajectories. In the first case, we call m a *counterclockwise* (CCW) motion. In the second case, we call it a *clockwise* (CW). All motions fall in at least one of the two categories, counterclockwise or clockwise. Therefore, our strategy consists in finding a feasible minimum-length motion in each of the two categories, and taking the best of both.

Given $r = r_{\mathbb{A}} + r_{\mathbb{B}}$ and two angles θ and θ', we define $d_r(\theta, \theta')$ as the width of the minimum strip containing any pair of points X and Y such that i) the bounding lines of the strip have slope $\theta + \pi/2$, ii) $\angle(X, Y) = \theta'$ and iii) Y lies on the boundary of $sq(X)$. Refer to Fig. 3.

Given an instance of our problem with $\theta_0 = \angle(A_0, B_0)$ and $\theta_1 = \angle(A_1, B_1)$, we define the function $s : [\theta_0, \theta_1] \to \mathbb{R}$ as $s(\theta) = \max_{\theta' \in [\theta_0, \theta_1]} d_r(\theta, \theta')$. $s(\theta)$ is a point-wise lower bound for $h_m(\theta)$ for any counterclockwise motion m. Intuitively, the idea is that any counterclockwise motion has to cover the angles from $\angle(A_0, B_0)$ to $\angle(A_1, B_1)$, and, for each of them, $s(\theta)$ gives the minimum valid distance between the centers of the two robots at that angle; hence, it is a lower bound for $h_m(\theta)$.

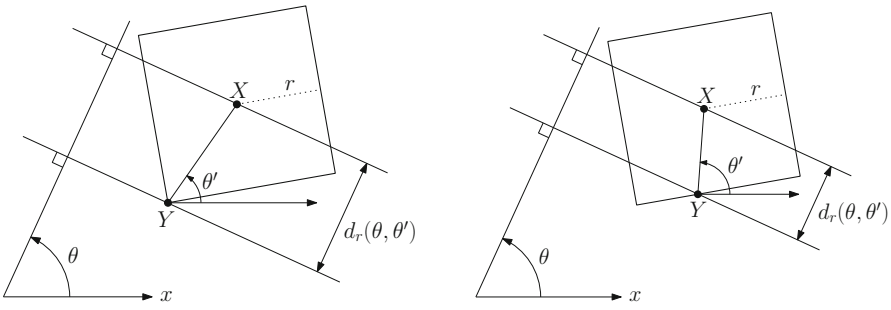

Fig. 3. Illustration of $d_r(\theta, \theta')$ for the same value of θ and two values of θ'.

Let $1_{[\theta_0,\theta_1]}$ be the indicator function of the interval $[\theta_0, \theta_1]$, and let $\overline{h}_m(\theta) = \overline{h}_{m_A}(\theta) + \overline{h}_{m_B}(\theta + \pi), \theta \in S^1$, where $\overline{h}_{m_A}(\theta)$ is the support function of the segment $\overline{A_0A_1}$, and $\overline{h}_{m_B}(\theta)$ is that of $\overline{B_0B_1}$. We define the lower bound function $LB : S^1 \to \mathbb{R}$ as $LB(\theta) = \max\{\overline{h}_m(\theta), s(\theta) \cdot 1_{[\theta_0,\theta_1]}\}$. Since for every angle θ the support function $h_{m_A}(\theta)$ (resp. $h_{m_B}(\theta)$) is lower-bounded by the support function $\overline{h}_{m_A}(\theta)$ (resp. $\overline{h}_{m_B}(\theta)$), we can then observe the following.

Observation 1. *If $m = (m_A, m_B)$ is a feasible counterclockwise motion from (A_0, B_0) to (A_1, B_1), then $h_m(\theta) \geq LB(\theta)$ for all $\theta \in S^1$.*

An analogous result holds for clockwise motions by replacing $1_{[\theta_0,\theta_1]}$ by $1_{S^1\setminus[\theta_0,\theta_1]}$ in the definition of function $LB(\theta)$. Finally, we present two conditions guaranteeing that the support function $h_m(\theta)$ coincides with $LB(\theta)$, hence implying that m has minimum length.

Lemma 1. *Let $m = (m_A, m_B)$ be a motion from (A_0, B_0) to (A_1, B_1). For any angle $\theta \in S^1$, if the support points for $h_m(\theta)$ are A_i and B_j, for $i, j \in \{0, 1\}$, then $h_m(\theta) = LB(\theta)$.*

Lemma 2. *Let $m = (m_A, m_B)$ be a motion from (A_0, B_0) to (A_1, B_1). For any angle $\theta \in [\theta_0, \theta_1]$, if the support points for $h_m(\theta)$ are one point X of m_A or m_B and a boundary point of its square $sq(X)$, then $h_m(\theta) = LB(\theta)$.*

Intuitively, what these conditions say is the following. Recall that by Cauchy's surface area formula, the length of a (convex) motion equals the integral of $h_m(\theta)$ over all angles θ. The first condition says that for a particular θ where the supporting lines are at an endpoint of motion m_A for robot $\mathbb{A}$ and at an endpoint of motion m_B for robot $\mathbb{B}$, the distance between the supporting lines has to be at least $\overline{h}_m(\theta)$. The second condition applies to the angles where the supporting lines are at a point X for one robot and at the boundary of $sq(X)$ for the other robot. In this case, the distance between the supporting lines has to be at least $s(\theta)$, achieved when one robot is sliding around the other one. Any smaller distance at that angle would imply a collision.

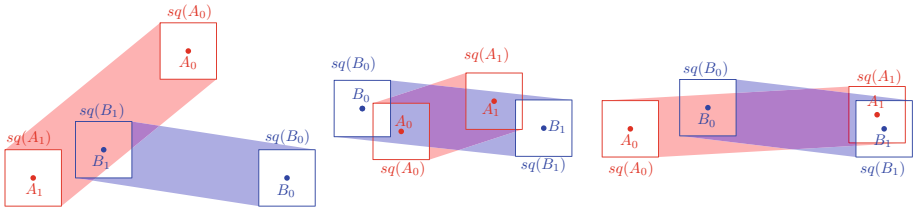

Fig. 4. Examples of corridors. Left: easy case, an optimal motion consists of first moving $\mathbb{A}$ straight, and then $\mathbb{B}$. Center: nested case. Right: multi-obstruction case. In the nested and in the multi-obstruction case an optimal motion requires first moving $\mathbb{A}$ to an intermediate position, then moving $\mathbb{B}$, and then again $\mathbb{A}$.

3 The Minimum-Length Motions at a Glance

In this section we make the minimum-length motions more precise. In particular, we claim that a minimum-length motion can always be obtained by sequentially and alternatively moving one robot at a time, in at most three movements.[2]

The *corridor* $corr_{\mathbb{A}}$ is the Minkowski sum of the closed line-segment $\overline{A_0A_1}$ and a square $sq(X)$, where X is the origin. The definition of $corr_{\mathbb{B}}$ is analogous. See Fig. 4, where $corr_{\mathbb{A}}$ is depicted in red and $corr_{\mathbb{B}}$ in blue.

The relative positions of A_0, A_1, B_0, B_1 with respect to $corr_{\mathbb{A}}$ and $corr_{\mathbb{B}}$ completely determine the shape of an optimal motion. Up to symmetry, exchanging the roles of $\mathbb{A}$ and $\mathbb{B}$, or exchanging the roles of A_0 by A_1, and B_0 by B_1, we can classify these relative positions in three types; see Table 1 and Fig. 4.

- *Easy*: $A_0 \notin corr_{\mathbb{B}}$ and $B_1 \notin corr_{\mathbb{A}}$.
- *Nested*: $A_0 \in corr_{\mathbb{B}}$, $A_1 \in corr_{\mathbb{B}}$, $B_0 \notin corr_{\mathbb{A}}$ and $B_1 \notin corr_{\mathbb{A}}$.
- *Multi-obstruction* (multi): $A_0 \in corr_{\mathbb{B}}$, $B_0 \in corr_{\mathbb{A}}$.

Our main result is summarized by the following theorem.

Theorem 2. *Let $\mathbb{A}$ and $\mathbb{B}$ be two axis-aligned square robots. Let their initial positions be A_0 and B_0, and their final positions be A_1 and B_1, respectively. Up to exchanging the roles of $\mathbb{A}$ and $\mathbb{B}$, there exists a position $A_{int} \notin sq(B_0) \cup sq(B_1)$ (possibly equal to A_0 or A_1) such that the following is a minimum-length feasible motion:*

1. *Move robot $\mathbb{A}$ along the shortest path from A_0 to A_{int} avoiding robot $\mathbb{B}$ (currently located at B_0).*
2. *Move robot $\mathbb{B}$ along the shortest path from B_0 to B_1 avoiding robot $\mathbb{A}$ (currently located at A_{int}).*
3. *Move robot $\mathbb{A}$ along the shortest path from A_{int} to A_1 avoiding robot $\mathbb{B}$ (currently located at B_1).*

[2] One movement is translating a robot from one point in the plane to another location where it does not intersect any other robot by minimizing the distance traveled.

Table 1. Exhaustive description of the cases.

	$A_0 \notin corr_{\mathbb{B}}$ $A_1 \notin corr_{\mathbb{B}}$	$A_0 \notin corr_{\mathbb{B}}$ $A_1 \in corr_{\mathbb{B}}$	$A_0 \in corr_{\mathbb{B}}$ $A_1 \notin corr_{\mathbb{B}}$	$A_0 \in corr_{\mathbb{B}}$ $A_1 \in corr_{\mathbb{B}}$
$B_0 \notin corr_{\mathbb{A}}$ $B_1 \notin corr_{\mathbb{A}}$	easy	easy	easy	nested
$B_0 \notin corr_{\mathbb{A}}$ $B_1 \in corr_{\mathbb{A}}$	easy	multi	easy	multi
$B_0 \in corr_{\mathbb{A}}$ $B_1 \notin corr_{\mathbb{A}}$	easy	easy	multi	multi
$B_0 \in corr_{\mathbb{A}}$ $B_1 \in corr_{\mathbb{A}}$	nested	multi	multi	multi

For each case (easy, nested, multi), the main challenges are i) defining an intermediate position A_{int} and ii) proving that the motion defined in Theorem 2 with that value of A_{int} is optimal.

We start by noting that in the easy case, an optimal motion consists of translating each of the robots directly from its initial to its final position along a straight-line segment, but the order might be relevant. In the remaining cases, a straight-line motion is not possible, so we need a finer analysis.

The full proof, covering the rest of the cases, requires the analysis of a large number of situations. Due to space limitations, in Sect. 4 we only explain in some detail the nested case. The remaining details can be found in the full version.

4 Details on Minimum-Length Motions for the Nested Case

In the following, it will be more convenient to assume, without loss of generality, that B_0 and B_1 are horizontally aligned; this can be achieved with a suitable rotation (note that in the figures that follow, squares have been rotated accordingly). Moreover, we will also assume that B_0 lies to the left of B_1, since otherwise a 180° rotation would take us to this situation. These assumptions are for ease of presentation, allowing us to properly use expressions like "upper tangent" as well as the notions "above", "below", "left" and "right".

Since we are in the nested case, without loss of generality, we can assume that $A_0, A_1 \in corr_{\mathbb{B}}$ and $B_0, B_1 \notin corr_{\mathbb{A}}$. Observe that $B_0, B_1 \notin corr_{\mathbb{A}}$ implies that $A_i \notin sq(B_j)$ for $i, j \in \{0, 1\}$.

Let t_{ij} denote the upper tangent line from a point A_i to $sq(B_j)$, for $i, j = 0, 1$. Let p_{ij} be the support point of line t_{ij} in $sq(B_j)$. We will consider t_{ij} as a directed line, directed from A_i to p_{ij}. We say that two tangents t_{i0} and t_{i1} are *twisted* if p_{i1} is to the left of t_{i0}, for some $i \in \{0, 1\}$. See Fig. 8, where tangents t_{00} and t_{01} are non-twisted, and Fig. 5, where t_{00} and t_{01}, and t_{10} and t_{11} are twisted.

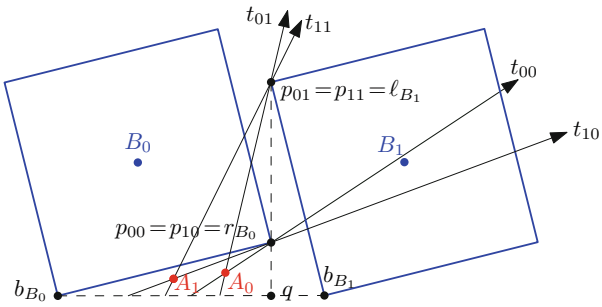

Fig. 5. t_{00} and t_{01}, and t_{10} and t_{11} are twisted. Note that A_1 and A_0 are below the polyline $b_{B_0} r_{B_0} q$.

We will use the notation $\overrightarrow{pq}$ to denote the line through p and q in the direction of the vector $q - p$. Note that t_{i0}, t_{i1} are twisted if A_i is to the right of the line $\overrightarrow{b_{B_0} r_{B_0}}$ and to the left of the line $\overrightarrow{p_{i0} p_{i1}}$.

For the nested case, we need to differentiate three cases, depending on whether the motion is *fully* CCW (i.e., it does not contain CW (sub)motion parts) or not, and, in the former case, depending on whether at least one of the pairs of tangents t_{i0}, t_{i1} is twisted or not.

In the following we only examine motions that are counterclockwise; a clockwise optimal motion can be obtained by reflecting the initial and final placements across the x-axis, and then computing an optimal counterclockwise motion.

4.1 Motion is Fully CCW, t_{00} and t_{01}, or t_{10} and t_{11} are Twisted

If the motion is fully CCW, but a pair of tangents t_{i0}, t_{i1} is twisted, the motion described in Theorem 2 might not be optimal. In this case, we prove that there exists a CW motion that is feasible and globally optimal, therefore we can ignore instances with twisted tangents.

If t_{i0} and t_{i1} are twisted, the sides of the squares are not axis-aligned. So, let $r_{B_i}, b_{B_i}, \ell_{B_i}$, and t_{B_i} be, respectively, the right, bottom, left, and top corner of $sq(B_i)$, for $i \in \{0, 1\}$. Let $r_{A_i}, b_{A_i}, \ell_{A_i}$, and t_{A_i} be, respectively, the right, bottom, left, and top corner of $sq(A_i)$, for $i \in \{0, 1, int\}$. Let q be the intersection between the lines $\overrightarrow{\ell_{B_1} r_{B_0}}$ and $\overrightarrow{b_{B_0} b_{B_1}}$; see Fig. 5. Then, we know the following:

Observation 3. *If t_{i0} and t_{i1} are twisted, A_i is below or on the polyline $b_{B_0} r_{B_0} q$ and above or on the line $\overrightarrow{b_{B_0} b_{B_1}}$. Hence, the highest point A_i could be is r_{B_0}, and the highest point ℓ_{A_i} and r_{A_i} could be is on the line $\overrightarrow{B_0 B_1}$. Also, since we are in the nested case, A_0 is visible from A_1.*

We will prove that if t_{00} and t_{01}, or t_{10} and t_{11} are twisted, there is a clockwise motion as short or shorter than any counterclockwise motion, for any possible position of the intermediate point A_{int} in the counterclockwise motion.

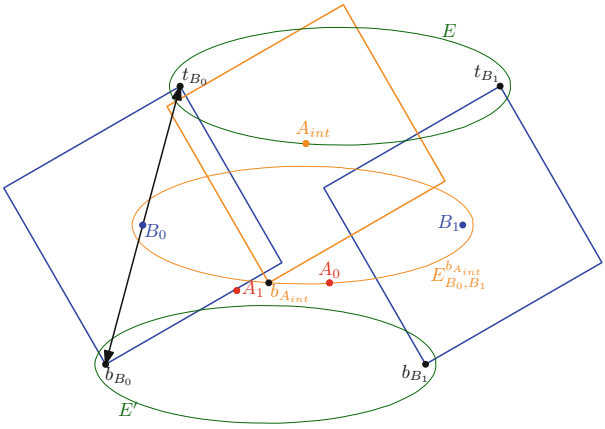

Fig. 6. Ellipse $E^{b_{A_{int}}}_{B_0,B_1}$ translated by the vectors $\overrightarrow{B_0 t_{B_0}}$ and $\overrightarrow{B_0 b_{B_0}}$.

Theorem 4. *In a fully counterclockwise motion, if t_{i0} and t_{i1} are twisted, for some $i \in \{0, 1\}$, then the minimum-length motion is clockwise.*

Proof. We will show that there is an intermediate position A'_{int} for the motion of $\mathbb{A}$ such that the length of motion m_B around A'_{int} in the CCW and in the CW motion is the same. In addition, we will need that the distance traveled by $\mathbb{A}$ in the CW motion is not larger than the distance traveled in the CCW motion.

Let $E^z_{x,y}$ denote the ellipse through z, whose two foci are x and y. We distinguish the case where $b_{A_{int}}$ belongs to the interior of both $E^{t_{A_0}}_{B_0,B_1}$ and $E^{t_{A_1}}_{B_0,B_1}$, and a second case where $b_{A_{int}}$ does not belong to the interior of one ellipse $E^{t_{A_j}}_{B_0,B_1}$, for some $j \in \{0, 1\}$.

Let E and E' be the ellipses $E^{b_{A_{int}}}_{B_0,B_1}$ translated by, respectively, the vectors $\overrightarrow{B_0 t_{B_0}}$, and $\overrightarrow{B_0 b_{B_0}}$; see the dark-green ellipses in Fig. 6. First, if $b_{A_{int}}$ belongs to the interior of both $E^{t_{A_0}}_{B_0,B_1}$ and $E^{t_{A_1}}_{B_0,B_1}$, by the construction of E' and the two robots having the same orientation, we know that E' does not contain A_0 nor A_1. Similarly, using Observation 3, and the construction of E, we know that it does not contain A_0 nor A_1.

Consider the point A'_{int} in E', which is the reflection of A_{int} about the segment $\overline{B_0 B_1}$ and then about its bisector; see Fig. 7. Using the symmetry of E and E', we get that $|A_i A'_{int}| + |A'_{int} A_{1-i}| \leq |A_{1-i} A_{int}| + |A_{int} A_i|$.

This means that the distance from A_0 to A_1 through A'_{int} is not larger than the distance through A_{int}. Thus, we found a position A'_{int} such that the distance traveled by $\mathbb{B}$ in the CCW motion around A_{int} is the same than the distance in the CW motion around A'_{int}. However, the distance traveled by $\mathbb{A}$ in the CW motion is not larger than the distance traveled in the CCW motion.

Similarly, let $j \in \{0, 1\}$ be such that $b_{A_{int}}$ does not belong to the interior of $E^{t_{A_j}}_{B_0,B_1}$. This case can be proved in a similar fashion, using Observation 3, and the properties of the ellipses. See the full version for more details. □

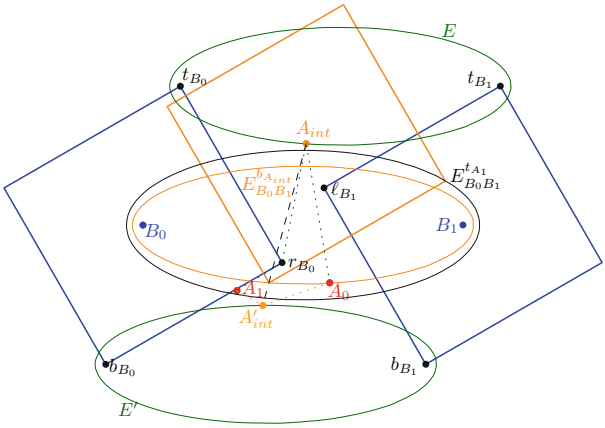

Fig. 7. A'_{int} belongs to the ellipse E', and the distance $|A_0A'_{int}| + |A'_{int}A_1|$ is shorter than the distance $|A_0A_{int}| + |A_{int}r_{B_0}| + |r_{B_0}A_1|$.

Theorem 4 allows us to ignore the case defined in this section, and the optimal motion will be obtained when analyzing the CW motion. It is worth noting that, since A_i is below the polyline $b_{B_0}r_{B_0}q$, and A_0 is visible from A_1, t_{i0} and t_{i1} cannot be twisted in the CW case if they are twisted in the CCW case.

4.2 Motion is Fully CCW, and no Tangents t_{i0} and t_{i1} are Twisted

If the motion is fully CCW, and no tangents are twisted, we prove that the sufficient conditions from Lemmas 1 and 2 are fulfilled, and that the motion is always feasible. To that end, we analyze the position of the two supporting lines for each possible angle $\theta \in [\theta_0, \theta_1]$, and argue that for each value of θ, either both supporting lines are touching A_i and B_j, for $i, j \in \{0, 1\}$, or one is touching a point X of one of the motions, and the other is touching its square $sq(X)$. This implies that the sufficient conditions hold, thus the motion is optimal. In addition, the motion is feasible since $A_{int} \notin (sq(B_0) \cup sq(B_1))$ and A_{int} is visible from both A_0 and A_1.

Let $vis(A_0)$ be the region of $corr_{\mathbb{B}} \backslash (sq(B_0) \cup sq(B_1))$ that is visible from A_0. $vis(A_0)$ is decomposed into four *zones*, defined by the tangents t_{ij}; see Fig. 8. For each zone we specify a different location for the intermediate point A_{int}. In this section we explain the case where A_1 belongs to Zone I, the locus of all points to the right of t_{00} and to the left of t_{01}, and defer to the full version the rest of the cases.

If $A_1 \in$ Zone I, $A_{int} = A_1$. Recall that $c_{m_A}(\theta)$ is the supporting line for $\overline{m}_A$ in direction $\theta + \pi/2$ and $c_{m_B}(\theta)$ is the supporting line for $\overline{m}_B$ in direction $\theta + \pi + \pi/2$. So, when the supporting point of $c_{m_B}(\theta)$ is B_j, the supporting point of $c_{m_A}(\theta)$ is A_i, for $i, j \in \{0, 1\}$ and the conditions from Lemma 1 are fulfilled. Hence, we just need to prove that when $c_{m_B}(\theta)$ is touching a corner of $sq(A_{int})$, $c_{m_A}(\theta)$ is touching $A_{int} = A_1$.

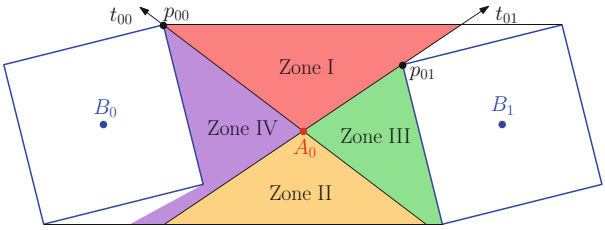

Fig. 8. Possible regions for A_1 in the nested case.

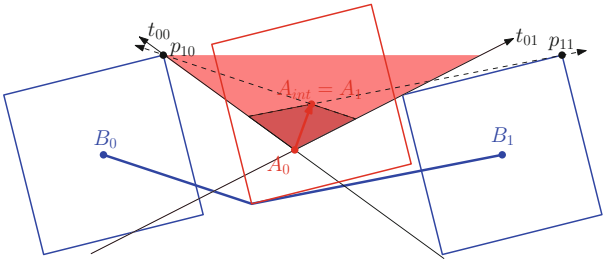

Fig. 9. A_0 has to be in the shaded region when $A_1 \in$ Zone I.

The first segment of the motion m_B is parallel to the line $\overrightarrow{A_1p_{10}}$, and the last segment is parallel to the line $\overrightarrow{A_1p_{11}}$; see Fig. 9. The motion of the supporting lines is counterclockwise, so we have to argue that from the moment $c_{m_B}(\theta)$ starts touching a corner of $sq(A_{int})$ until it stops touching a corner of $sq(A_{int})$, $c_{m_A}(\theta)$ is touching A_1. This is analogous to showing that from the moment $c_{m_A}(\theta)$ touches p_{10} until it touches p_{11}, $c_{m_A}(\theta)$ does not touch A_0, i.e., that A_0 is on or below the *lower envelope*[3] of the lines $\overrightarrow{A_1p_{10}}$ and $\overrightarrow{A_1p_{11}}$. One can prove this property by using the fact that both supporting lines are parallel, and the definition of Zone I.

4.3 Motion Contains CW Parts

If the motion contains clockwise (sub)motion parts, there can be some angles for which the motion does not satisfy any of the two sufficient conditions from Lemmas 1 and 2. This means that the techniques used previously to prove the optimality of the motions cannot be directly applied. However, we show in the full version that in such a case, there exists an alternative motion m', which is different in the coordination scheme from m, but that is fully counterclockwise and has exactly the same trace for $\mathbb{A}$ and $\mathbb{B}$ (thus also the same length). Since m' is fully counterclockwise, we can apply the results in Sects. 4.1 and 4.2 to prove that m' has minimum length. Therefore, since m has the same length as m', we can conclude that m is optimal as well.

[3] If we think of a finite set of lines as graphs of (partially defined) functions, the lower envelope is the graph of the pointwise minimum [12].

5 Conclusions

We have presented a full description of minimum-length coordinated motions for two axis-aligned square robots translating in an obstacle-free plane. This is a fundamental problem in motion planning, and an important step to design algorithms that can produce high-quality motions for more complex situations involving obstacles.

While our work builds on top of the tools developed for disc robots [7,8], we show that squares present several additional difficulties over the case of discs. Moreover, we present a full analysis of all cases that arise, with complete details, many of which had not been treated in previous work.

Our full characterization of optimal coordinated motions for two square robots opens several roads for future research. Moreover, we expect that the techniques developed in this work can be generalized to robot shapes other than squares, especially regular polygons. Dealing with non-axis aligned square robots would be another interesting extension, but it may require important changes to our proofs, since they rely heavily on the parallelism of square edges. Another natural question is how to extend this work from two to three (or more) robots. Finally, as already mentioned, the addition of obstacles, even for just two robots, is probably the most relevant next step.

References

1. Choset, H., et al.: Principles of Robot Motion: Theory, Algorithms, and Implementation. MIT Press, Cambridge (2005)
2. Dubins, L.E.: On curves of minimal length with a constraint on average curvature, and with prescribed initial and terminal positions and tangents. Am. J. Math. **79**, 497–516 (1957)
3. Eggleston, H.G.: Convexity (1966)
4. Halperin, D., Kavraki, L., Solovey, K.: Robotics. In: Goodman, J.E., O'Rourke, J., Tóth, C., (eds.), Handbook of Discrete and Computational Geometry, chapter 51, pp. 1343–1376. 3rd edn Chapman & Hall/CRC (2018)
5. Halperin, D., Salzman, O., Sharir, M.: Algorithmic motion planning. In: Goodman, J.E., O'Rourke, J., Tóth, C., (eds.) Handbook of Discrete and Computational Geometry, chapter 50, pp. 1311–1342. 3rd edn Chapman & Hall/CRC (2018)
6. Icking, C., Rote, G., Welzl, E., Yap, C.: Shortest paths for line segments. Algorithmica **10**(2), 182–200 (1993)
7. Kirkpatrick, D.G., Liu, P.: Characterizing minimum-length coordinated motions for two discs. In Proceedings of 28th CCCG, pp. 252–259 (2016)
8. Kirkpatrick, D.G., Liu, P.: Characterizing minimum-length coordinated motions for two discs. CoRR, abs/1607.04005 (2016). http://arxiv.org/1607.04005
9. Latombe, J.-C.: Robot Motion Planning. Kluwer, Boston (1991)
10. Latombe, J.-C.: Motion planning: a journey of robots, molecules, digital actors, and other artifacts. Int. J. Robot. Res. **18**(11), 1119–1128 (1999)
11. Steven, M.: LaValle. Cambridge University Press, Planning Algorithms (2006)
12. Matousek, J.: Lectures on Discrete Geometry, vol. 212. Springer, Cham (2013)

13. Mitchell, J.S.B.: Shortest paths and networks. In: Goodman, J.E., O'Rourke, J., Tóth, C., (eds.), Handbook of Discrete and Computational Geometry, chapter 31, 3rd edn., pp. 811–848. Chapman & Hall/CRC (2018)
14. Reeds, J.A., Shepp, L.A.: Optimal paths for a car that goes both forwards and backwards. Pac. J. Math. **145**(2), 367–393 (1990)
15. Salzman, O.: Sampling-based robot motion planning. Commun. ACM **62**(10), 54–63 (2019). https://doi.org/10.1145/3318164
16. Sharir, M., Sifrony, S.: Coordinated motion planning for two independent robots. Ann. Math. Artif. Intell. **3**(1), 107–130 (1991). https://doi.org/10.1007/BF01530889
17. Solovey, K., Halperin, D.: On the hardness of unlabeled multi-robot motion planning. Int. J. Robot. Res. **35**(14), 1750–1759 (2016). https://doi.org/10.1177/0278364916672311